A peer-reviewed version of this preprint was published in PeerJ on 13 December 2016.

Strehlow BW, Jorgensen D, Webster NS, Pineda M, Duckworth A. 2016. Using a thermistor flowmeter with attached video camera for monitoring sponge excurrent speed and oscular behaviour. PeerJ 4:e2761 https://doi.org/10.7717/peerj.2761

Integrating a thermistor flowmeter and time lapse imagery to monitor sponge (Porifera) behaviour

Brian W Strehlow Corresp., [1, 2, 3] , **Damien Jorgensen** [3] , **Nicole S Webster** [3] , **Mari-Carmen Pineda** [2, 3] , **Alan Duckworth** [2, 3]

[1] School of Plant Biology; Centre for Microscopy, Characterisation and analysis; and Oceans Institute, Universtiy of Western Australia, Crawley, WA, Australia
[2] Western Australian Marine Science Institution, Crawley, WA, Australia
[3] Australian Institute of Marine Science, Townsville, QLD, Australia

Corresponding Author: Brian W Strehlow
Email address: brian.strehlow@research.uwa.edu.au

A digital, four-channel thermistor flowmeter was developed as an experimental tool for measuring pumping rates in marine sponges, particularly those with small excurrent pores (oscula). The flowmeter is integrated with time lapse cameras and has an accuracy of ±5 mm s^{-1} over the range of 5–200 mm s^{-1}, a spatial resolution of 1.4 mm, and an adjustable temporal resolution of 5 seconds. Combining flowmeters with time lapse imagery yielded valuable insights into the contractile behaviour of oscula in *Cliona orientalis,* revealing four distinct oscula states: (1) osculum open with extended papilla, (2) osculum closed with extended papilla, (3) osculum closed with papilla retracted, and (4) osculum closed with papilla retracted and contraction of region surrounding osculum. Osculum area was positively correlated to measured excurrent velocities, indicating that sponge pumping and osculum contraction are coordinated behaviours. Diel trends in pumping activity and osculum contraction were also observed, with sponges increasing their pumping activity to peak at midday and decreasing pumping and contracting oscula at night. Short-term elevation of the suspended sediment concentration within the seawater initially decreased pumping rates by up to 90%, ultimately resulting in closure of the oscula and cessation of pumping. The thermistor flowmeter developed here will be a valuable tool to monitor behaviour, physiology and ecophysiology of sponges.

Integrating a thermistor flowmeter and time lapse imagery to monitor sponge (Porifera) behaviour

Brian W. Strehlow[1,2,3,4], Damien Jorgensen[3], Nicole S. Webster[3,4], Mari-Carmen Pineda[3,4], Alan Duckworth[3,4]

[1]School of Plant Biology, University of Western Australia, Crawley, WA, Australia

[2]Centre for Microscopy Characterisation and analysis, University of Western Australia, Crawley, WA, Australia

[3]Australian Institute of Marine Science, Townsville, QLD, Australia

[4]Western Australian Marine Science Institution, Crawley, WA, Australia

Corresponding author:

Brian Strehlow[1,2,3,4]

Australian Institute of Marine Science (AIMS), PMB3, Townsville, QLD, 4810, Australia

E-mail: brian.strehlow@research.uwa.edu.au

PeerJ Preprints | https://doi.org/10.7287/peerj.preprints.2137v1 | CC BY 4.0 Open Access | rec: 16 Jun 2016, publ: 16 Jun 2016

Abstract

A digital, four-channel thermistor flowmeter was developed as an experimental tool for measuring pumping rates in marine sponges, particularly those with small excurrent pores (oscula). The flowmeter is integrated with time lapse cameras and has an accuracy of ±5 mm s^{-1} over the range of 5–200 mm s^{-1}, a spatial resolution of 1.4 mm, and an adjustable temporal resolution of 5 seconds. Combining flowmeters with time lapse imagery yielded valuable insights into the contractile behaviour of oscula in *Cliona orientalis,* revealing four distinct oscula states: (1) osculum open with extended papilla, (2) osculum closed with extended papilla, (3) osculum closed with papilla retracted, and (4) osculum closed with papilla retracted and contraction of region surrounding osculum. Osculum area was positively correlated to measured excurrent velocities, indicating that sponge pumping and osculum contraction are coordinated behaviours. Diel trends in pumping activity and osculum contraction were also observed, with sponges increasing their pumping activity to peak at midday and decreasing pumping and contracting oscula at night. Short-term elevation of the suspended sediment concentration within the seawater initially decreased pumping rates by up to 90%, ultimately resulting in closure of the oscula and cessation of pumping. The thermistor flowmeter developed here will be a valuable tool to monitor behaviour, physiology and ecophysiology of sponges.

Introduction

Sponges (Porifera) are generally considered ‘simple’ animals, yet they have surprisingly complex physiologies. Sponges actively pump water through their tissues using specialised chambers of flagellated cells called choanocytes. They depend on water circulation for food

capture, waste elimination, gas exchange and reproduction (Bergquist 1978). Water is pumped through small incurrent pores (ostia) to a system of channels leading to chambers full of choanocytes before flowing out larger excurrent pores (oscula) (Bergquist 1978). Due to the variability in morphologies and trophic strategies, generalisations about sponge pumping behaviours are difficult. Different studies have shown that sponge pumping is variable. Pumping can be continuous, periodic (diurnally or seasonally), or exhibit random cessations, depending on the species (Reiswig, 1971; Gerrodette & Flechsig, 1979; Tompkins-MacDonald & Leys, 2008; McMurray, Pawlik & Finelli, 2014).

Since there is considerable inter-species variation in pumping activities, accurate quantification of the excurrent flow rate from oscula is critical to understanding sponge physiology and ecology. In the past, various filming methods have been used, including manually tracing plumes of fluorescent dye over a set distance (Weisz, Lindquist & Martens, 2008; Massaro et al., 2012) and laser tracking of displaced particles around oscula (e.g. Mendola et al., 2007). Processing video footage is time consuming and the temporal resolution can be very low for video tracing, especially *in situ* where SCUBA diving limits observation periods. Furthermore, the addition of experimental stressors such as suspended solids could potentially confound results by limiting visibility. Pumping rates may also be measured by isolating the excurrent flow in a tube and observing dye movement through the tube (Gerrodette & Flechsig, 1979); however, this limits measurement to sponges with large oscula. Prolonged obstruction of oscula with probes or tubing can also cause new adjacent oscula to form in some species (Strehlow pers. obs. in *Cliona orientalis* and *Rhopaloides odorabile*), and flow isolation techniques may only be compatible with sponges that have large, non-contractile oscula. Acoustic Doppler velocimetry (ADV) is an excellent method for flow measurements of sponges with oscula larger than 3–4 cm (McMurray,

Pawlik & Finelli, 2014) as it provides high spatial and temporal resolution *in situ*. However, many sponges have oscula too small to be accurately measured using ADVs.

Thermistor flowmeters offer an alternative approach for flow quantification, particularly for species with small oscula. Thermistor flowmeters use heat dissipation as a proxy for flow. The thermistor probe heats up to a specific temperature, and the power supplied to the probe is varied in order to keep the probe at this constant temperature. The amount of power required to maintain the elevated temperature is correlated to the water flow experienced by the heated thermistor, with higher flows corresponding to greater heat loss from the probe head. McCammon (1965) first used heated thermistors to measure pumping rates of bivalves, and Reiswig (1971) and Mackie et al. (1983) subsequently used them with sponges. Thermistors improved significantly in the digital age, decreasing in size from ~5 mm (Labarbera & Vogel 1976) to ~1 mm using commercially available probe tips (Tompkins-MacDonald & Leys, 2008; Schläppy et al., 2010). This size range makes thermistor flowmeters ideal for quantifying pumping rates in multiple sponge taxa.

Understanding sponge behaviour is critical to accurate pumping rate quantification as some species can actively open and close their ostia and oscula (Harrison, 1972; Weissenfels, 1976; Ilan & Abelson, 1995; Leys & Meech, 2006; Elliott & Leys, 2007); expand and contract their whole bodies (Nickel, 2004; Ellwanger & Nickel, 2006; Nickel et al., 2011); and execute coordinated behaviour patterns (Ludeman et al., 2014). In the current study, a multi-channel digital thermistor flowmeter was developed that incorporated time-lapse cameras to observe behaviour in the common, Indo-Pacific bioeroding sponge *Cliona orientalis* (Thiele, 1900). ‘Cliona’ is derived from the Greek ‘claudo’, which means to close. The position of Clionid sponges on the tree of life historically baffled scientists as their compositional relationship to sponges belied their observed contractile responses to mechanical stimuli

(Grant, 1826). The relationship between excurrent velocities and oscular diameter during contractions in *C. orientalis* was examined. It was hypothesized that there would be a direct correlation between the two. The thermistor flowmeter apparatus was also used to determine the pumping and contractile responses of *C. orientalis* to elevated suspended sediment concentrations (SSCs). Previous studies have shown that pumping rates in sponges significantly decrease when exposed to elevated SSCs (Gerrodette and Flechsig, 1979; Leys et al., 1999; Reiswig, 1971; Tompkins-MacDonald and Leys, 2008). Although this response has not been examined in *C. orientalis*, it was hypothesized that pumping rates would decrease in response to elevated SSCs.

Materials and Methods

1.1 Thermistor flowmeter construction and calibration

The thermistor flowmeter was designed and built at the Australian Institute of Marine Science (AIMS) in Townsville (Queensland, Australia), with all testing done at the AIMS National Sea Simulator (SeaSim). The flowmeter incorporated four thermistor probes and a thermometer to determine ambient temperature. Each glass thermistor probe (120 series, 1000Ω at 25 °C, Honeywell, USA) was set to hold at 10°C above ambient temperature. In high flow conditions the probes drew more power to maintain this temperature difference hence power could be directly correlated to flow rate. All calculations were performed within a Microchip PIC microcontroller. Data analogue to digital conversion was done with a 16-bit Analog Devices AD7706 analogue to digital converter, which is interfaced to a Microchip PIC18F2525 microcontroller (Fig. 1). Thermistor voltage was controlled via a 16-bit Texas Instruments DAC8411 digital to analogue converter. Data from each heated thermistor ran through the PIC microcontroller's PUART interface, and passed via a FTDI TTL to USB

converter cable to a computer. Custom software, written in Visual Basic, received data, displayed it graphically and saved it as a text file. The circuit boards and USB hub were compacted and placed into a splash-proof Pelican case.

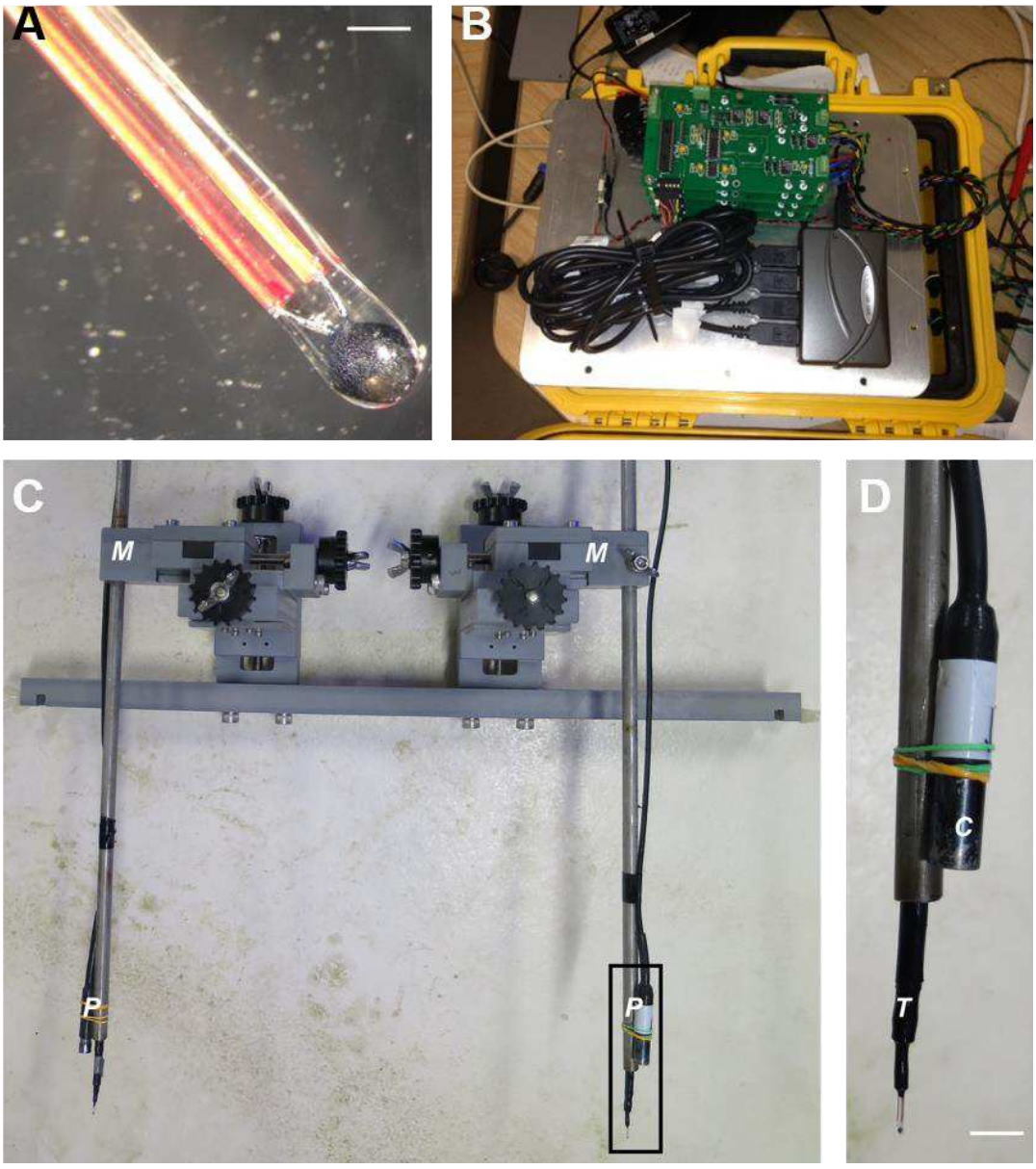

Figure 1. A. Probe tip (scale = 1 mm). B. Circuit boards that control each of four probes connected to USB. All circuitry fits into a waterproof Pelican case. C. Two thermistor probes. The micromanipulator (*M*) is secured across the tank to limit vibration. Each of the two probe tips (*P*) can be moved in three dimensions using the large, black screw heads. D. A close up of the rectangle denoted in the bottom right of panel C with thermistor head (*T*) and USB camera (*C*) used for positioning and measuring oscula diameter. Scale bar is 5 mm.

Calibration of the thermistor (to determine relationship between heat loss and water flow) was first attempted by placing each heated probe in the outlet of a pipe. However, flow speeds across the pipe were not uniform and the process resulted in different values depending on where each thermistor was placed in the pipe. A more accurate calibration method was developed by pulling each thermistor on a track through a 3 m long tank of seawater. Each probe was placed on a frame attached to a carriage running along a rail on top of the tank and driven by a stepper motor through a belt and pulley system. This optimised calibration method facilitated accurate and stable control of flow across the probe.

In order to create a calibration curve for each probe, the thermistor was run across the track at 13 different speeds from 5 to 200 mm s^{-1}. Three calibration runs were performed for each speed, and the power used to maintain thermistor temperature was averaged across the three trials. The waterproofing used on the glass coating on the probes caused slightly different readings between probes, necessitating a separate calibration curve for each unit. To confirm precision at different temperatures, the same calibration runs were performed at different temperatures (24–29˚C at 1˚C intervals). Curves were fitted to a polynomial regression model for power compensation developed by Moore (2003) using R64 (R core team, 2015). All subsequent recalibration runs were performed using 8 speeds.

1.2 Testing for influence of suspended sediments on probe readings

Probes were tested to verify that elevated SSCs did not interfere with water flow measurements. Tests were conducted in 100 L tanks filled with 27°C, 5 µm filtered seawater flowing in at 600 mL min^{-1} to ensure 8 turnovers per day. To help keep sediments in suspension and reduce deposition, water in each tank was recirculated using an Iwaki MD

magnetic drive centrifugal pump (Iwaki Pumps, Australia) that collected water from the surface and forced it up through the centre point of the inverted pyramid at the tank's base. Tank circulation and SSC suspension was further maintained with a VorTech MP40 pump (EcoTech Marine, USA) mounted on the tank's upper sidewall. Sediments were prepared from biogenic calcium carbonate sediment collected from Davies Reef (a clear-water, mid-shelf reef in the central Great Barrier Reef). Sediment was dried and ground using a rod mill grinder until the mean grain size was ~29 µm with 80% of the sediment ranging in size between 3 and 64 µm, as measured using laser diffraction techniques (Mastersizer 2000, Malvern Instruments Ltd, UK).

In order to determine the effect of sediments on flow measurements, probe readings were compared at the same positions in tanks under the following three conditions: (i) sediment was directly deposited onto the probe tips, (ii) probe tips were cleaned and (iii) sediment was in suspension but an observable layer had not yet deposited on the probe tips. The first condition was achieved by allowing sediment to deposit on the tip of the probe for one day after a single pulse of 100 mg L^{-1}. This level was chosen to reflect SSC within 500 m of dredging activities, where SSCs can range from 100–300 mg L^{-1} for periods of several hours (Jones et al., 2015). Ambient flow was then measured for each of the probes for approximately 30 min. Flow rates were calculated and logged every five seconds (n=385). Probes were subsequently cleaned of sediment without changing their position using gentle bursts of water from a plastic transfer pipette. Measurements were recorded in the same position for a further 30 min in this clean state. Finally, a single pulse of sediment was added to establish a SSC of 100 mg L^{-1}. Mean flow rates for each condition (unclean, clean and sediment) were compared using one-way ANOVAs for each probe using SigmaPlot Version

11.0 (Systat Software Inc.). In order to meet assumptions of normality, ANOVAs were run on ranks.

1.3 3D profiling of sponge flow

Small sponge explants (50 mm in diameter and containing several oscula) were drilled using a compressed air drill from large colonies of *C. orientalis* inhabiting the skeleton of dead *Porites* sp. coral. Explants were collected at 3 m depth from reefs around Pelorus Island (S 18°32.903' E 146° 29.172', Permit: G12/35236). Explants were acclimated to aquarium conditions for two weeks before experimentation. Waterproof USB endoscopes (7mm USB waterproof endoscope, Snake Inspection Cameras, China) aided in accurate positioning of the probes over the oscula (Fig. 1C). In order to test the spatial resolution of the thermistor, 3D flow patterns were measured for a single osculum. The probe was positioned using a custom manipulator in 1 mm increments in the X, Y and Z directions at 60 locations in three dimensions around the sponge (Fig. 1A). Measurements were taken for one minute at each location. To decrease background noise, in-tank circulation was stopped during measurements. Sponge pumping was plotted in three dimensions using the plot3D package in R64 (R core team 2015).

1.4 Observations of oscular behaviour and excurrent velocity

The oscula of *C. orientalis* exhibited four distinct behavioural states: (1) osculum open with extended papilla (tissue projection around osculum); (2) osculum closed with papilla extended; (3) osculum closed and papilla retracted; and (4) osculum closed and papilla retracted with contraction of region surrounding osculum. The relationship between oscular state and sponge pumping was examined by measuring excurrent flow and osculum area every 5 s for 10 min. Two oscula were monitored. One osculum was in state 1, and the

second was transitioning from state 1 to 3. The osculum area, assuming a circular oscula, was based on the maximum diameter of the osculum as measured by ImageJ (Schneider et al 2012). Tank parameters used for this experiment were the same as those listed in section 1.2. A linear regression was performed using R64 (R Core Team, 2015) to relate osculum area to excurrent velocity. Excurrent velocities for state 4 were also recorded, and at these times, the oscula area was zero.

1.5 Effects of elevated SSC on pumping rates and osculum behaviours

Thermistor probes were positioned 1 mm above a single osculum of four sponges. To obtain 'normal' pumping rates unaffected by sediment, excurrent velocities from each sponge were measured for 30 min. Each sponge explant was exposed to a single pulse of sediment (100 mg L^{-1} added gradually over the course of five minutes) and then monitored for 3.5 h. The SSC was monitored using a nephelometer (TPS, Australia), and sedimentation rates were measured using SedPods (Field, Chezar & Storlazzi, 2013). SedPods were capped and any trapped or accumulated sediment determined gravimetrically. Sediment samples were filtered through pre-weighed 0.4 µm 47 mm diameter polycarbonate filters, incubated at 60°C for 24 h, and weighed to determine sediment mass, i.e. deposition. Oscula behaviour was monitored throughout the experiment using time lapse images taken every 5 s. Each of the four trials was independent, and the tanks were cleaned between trials. For consistency, each trial was conducted at the same time of day. SSCs in each tank was measured every ten minutes using a nephelometer (TPS, Australia) and nephelometric turbidity units (NTUs) converted to SSCs (as mg L^{-1}) by applying by a sediment-specific conversion factor based on the relationship between gravimetrically determined total suspended solid levels versus NTU.

A second experiment using the same approach was performed in which pumping rates and oscular behaviours were recorded for a different group of four explants for 2.5 d before and after three separate sediment pulses, each applied over a 4 h period. To prevent sediment deposition on the thermistor probes affecting flow measurements, each probe was carefully cleaned twice daily using a slow pulse of water from a plastic pipette. Tank temperature maintained at 27 ± 0.2˚C during the experiment.

Results

1.1 Calibration

While exponential correlations fit well for the middle values of the calibration runs, trends broke down at speeds greater than 110 mm s^{-1}. Curves were therefore fitted to a polynomial regression model to compensate for the levelling off in average power in each probe at higher speeds. The polynomial regression was a better fit for the higher range, increasing the instruments accuracy to 200 mm s^{-1} (Fig. 2). R-squared values for all four probes calibrated at four temperatures were greater than 0.99 (Table 1).

222 Table 1. Calibration curve polynomial regression summaries for probes 1–4 at 27˚C and
223 28˚C. Variables A through D represent coefficients to the polynomial regression.

224

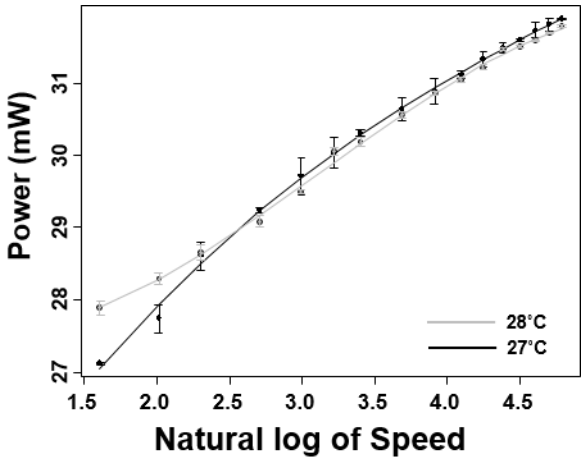

Figure 2. Example calibration curves for a single probe at 27˚C (black symbols) and 28 ˚C (white symbols). Data are mean ± SD of n = 3 calibration runs.

Table 1. Calibration curve polynomial regression summaries for probes 1–4 at 27˚C and 28˚C. Variables A through D represent coefficients to the polynomial regression.

Flow to power equation:		Power (mW) = A + B × ln(flow) + C × ln(flow)^2 + D × ln(flow)^3								
Temperature (˚C)	Probe	A	B	C	D	Multiple R^2	Adjusted R^2	F stat	Df	P
27	1	38.81	3.249	-0.3959	0.02141	0.996	0.9956	1505	3,17	< 0.01
27	2	34.40	3.682	-0.4949	0.03058	0.998	0.9976	2810	3, 17	< 0.01
27	3	26.35	2.816	-0.3302	0.01879	0.996	0.9955	1484	3, 17	< 0.01
27	4	32.29	6.201	-0.6858	0.04203	0.996	0.9951	1344	3, 17	< 0.01
28	1	28.73	-0.05767	0.4339	-0.05153	0.997	0.964	1377	3, 12	< 0.01
28	2	25.22	0.07463	0.3344	0.03963	0.999	0.9982	2727	3, 12	< 0.01
28	3	29.91	-0.5293	0.6638	-0.07507	0.998	0.9974	1934	3, 12	< 0.01
28	4	28.08	-1.279	0.8716	-0.09271	0.998	0.9976	2115	3, 12	< 0.01

225

226 In order to calculate flow, a successive approximation method based on the calibration
227 curve was used to back-calculate flow rate from power output. Custom designed software
228 facilitated modification of the calibration equations according to temperature. Importantly,
229 probe values designated ‘no flow’ are not actually zero due to the nature of the model and
230 the probes. Since the probes are heated, they create a small convection current under no

231 flow conditions. The convection currents were shown to be negligible (ranging from 0.5–1.0
232 mm s^{-1}). Power output under these 'no flow' conditions was higher than output under flow
233 <2.5 mm s^{-1} and the software reports a zero value in these cases. Hence the minimum flow
234 needed for accurate quantification was approximately 5 mm sec^{-1}. The reliable range of the
235 instrument was therefore defined as 5 to 200 mm s^{-1} with an accuracy of ± 5 mm s^{-1}.

236 As a consequence of having the probes heated to 10˚C above the ambient temperature,
237 no clear trend could be determined between ambient temperature and power, with curves
238 from different temperatures intersecting at two points. Differences in flow of 5 mm s^{-1} were
239 recorded if temperatures changed by 1°C. Experiments were therefore conducted at a
240 carefully controlled temperature for which a specific calibration curve was generated. As the
241 logging software records changes in temperature to ± 0.01˚C, experiments can be monitored
242 effectively and quality controlled with experiments aborted if temperatures changed by 0.5
243 ˚C.

244

245 1.2 Testing for influence of suspended sediments on probe readings

246 All clean probes had higher flow readings under constant, ambient flow than those
247 coated with sediment ($P<0.001$; Fig. 3). Sediment deposition on the probes 24 h after a
248 single dose of 100 mg L^{-1} interfered with the probe reading in both the high and low ambient
249 flow areas of the tank. Cleaning with submerged transfer pipettes did not alter the position
250 of the probes. Suspended sediment significantly decreased flow readings in all probes
251 ($P<0.001$) except probe 4; however, this decrease was very small (1.50 ± 0.40 mm s^{-1}, mean ±
252 SD). These differences were within the calibrated resolution of the instrument (5 mm s^{-1});

PeerJ Preprints | https://doi.org/10.7287/peerj.preprints.2137v1 | CC BY 4.0 Open Access | rec: 16 Jun 2016, publ: 16 Jun 2016

253 nevertheless, the effect was accounted for in future experiments to ensure accuracy of the
254 physiological measurements.

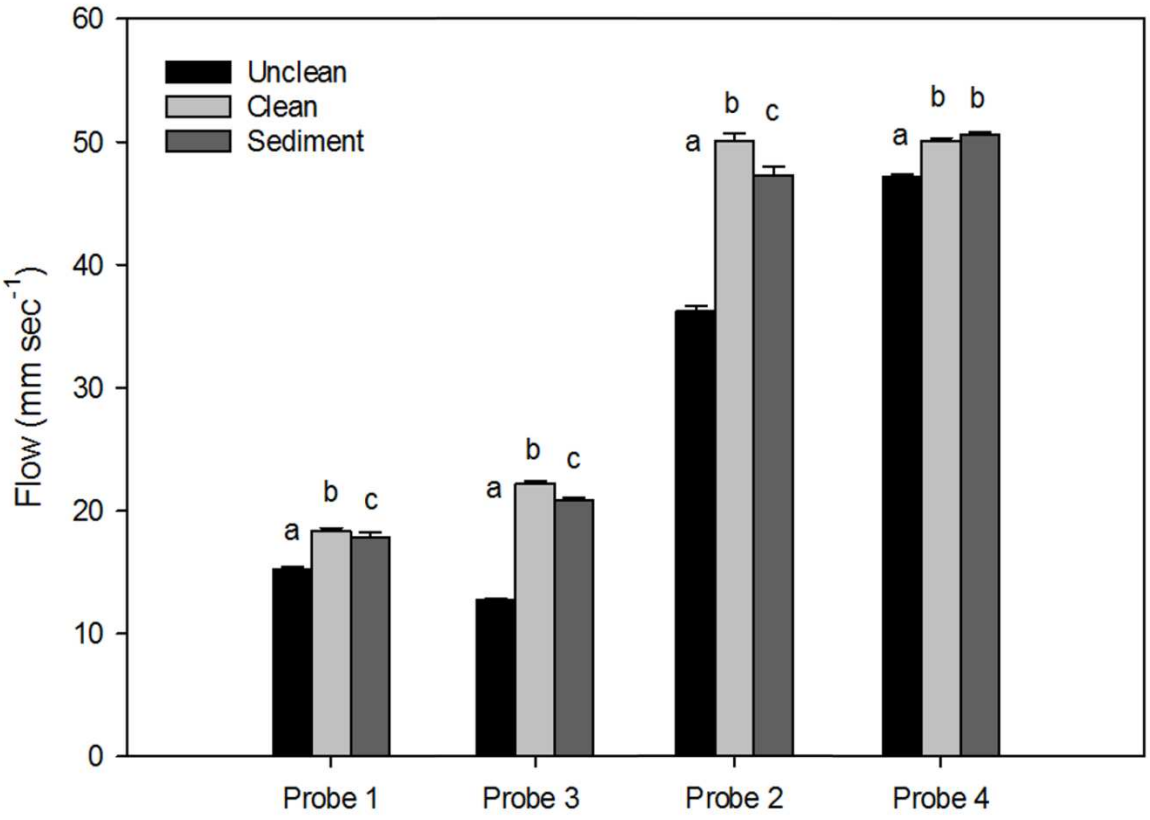

Figure 3. Comparison of flow readings for each probe under constant low flow rates (Probe 1 and 3) and high flow rates (Probe 2 and 4), before cleaning (i.e. with deposited sediment), after cleaning and after exposure to suspended sediments (± SE). Groups a, b and c are significantly different for each probe ($P<0.01$).

255 1.3 3D profiling of sponge flow

256 The spatial resolution of the thermistor was assessed by making small (2 mm) changes in
257 probe position around an osculum (Fig. 4A) to create a three dimensional 'flowscape' (Fig.
258 4B). The instrument detected changes in flow rates down to a spatial scale of 1 mm;
259 however, since the probe diameter is 1.4 mm, the spatial resolution of each probe was set at

PeerJ Preprints | https://doi.org/10.7287/peerj.preprints.2137v1 | CC BY 4.0 Open Access | rec: 16 Jun 2016, publ: 16 Jun 2016

1.4 mm. The flowscape was used to determine optimal probe positioning, which was directly in the centre of the osculum opening, approximately 1 mm above the surface. This positioning allowed the osculum to contract without interference from the probe. Contractile response in the osculum occurred when the probe was closer or touched the osculum. Flow <1 mm from the surface of the sponge, but not over the osculum, was <5 mm s^{-1}. Since ambient flow regimes were constant 4 mm away from the osculum in any direction, these values were used to zero excurrent velocities. The average flow recorded above the surface of the sponge, but not over the osculum, was subtracted from the excurrent velocity to zero values in subsequent experiments.

PeerJ Preprints | https://doi.org/10.7287/peerj.preprints.2137v1 | CC BY 4.0 Open Access | rec: 16 Jun 2016, publ: 16 Jun 2016

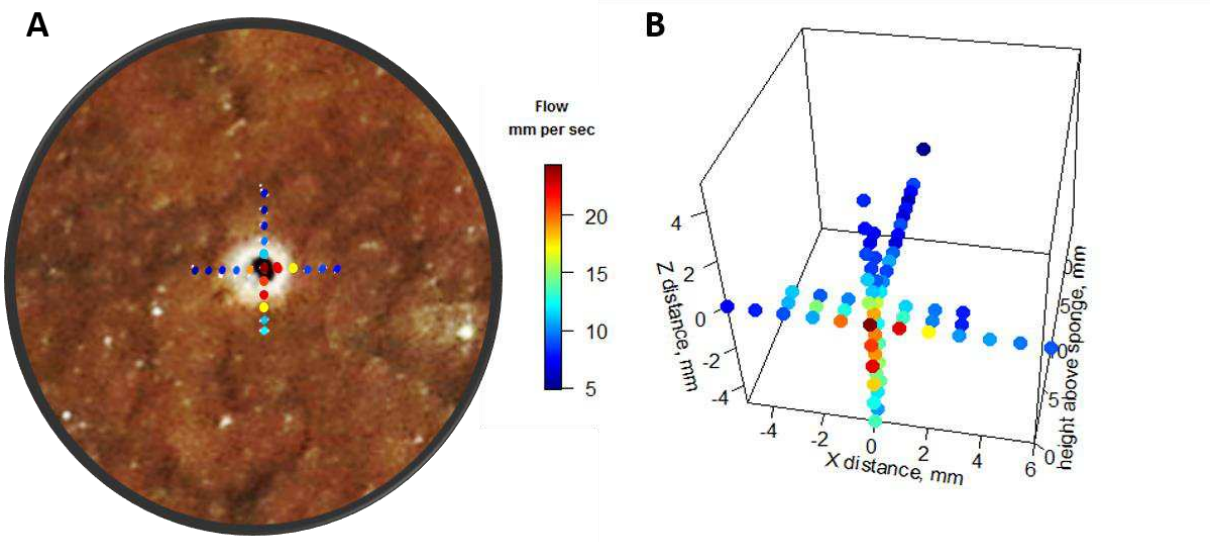

Figure 4. Demonstration of three dimensional measurement of sponge flow. Panel A shows the osculum (excurrent pore) of *Cliona orientalis*. The overlay shows the flow measured approximately one millimetre above the osculum at different positions on the X and Z axes. Flow rates were measured in mm s^{-1} and represented by colour according to the legend in the centre of the figure. Panel B shows the complete 3D flow dataset. Flow rates were measured for multiple X, Y and Z positions in mm increments, with the origin centred at a point 1 mm above the centre of the osculum.

1.4 Observations of oscular behaviour and excurrent velocities

Using time lapse imagery, four distinct osculum states were observed. State 1 was the result of 'normal' pumping (Fig. 5). In this condition oscula remained open but changed shape slightly due to ambient currents or, perhaps, turbulent flow from the osculum. In state 2, the oscula closed but the papillae remained extended, and excurrent flow was zero. This behaviour occurred several times per day. Excurrent velocities in state 3, i.e. oscula closed and papilla retracted (Fig. 5D), and 4, in which the area around the oscula was also contracted (Fig. 5F) were also zero. State 3 occurred in response to tactile stimulation of the oscula. *C. orientalis* oscula are sensitive to mechanical disturbance and may close, for

PeerJ Preprints | https://doi.org/10.7287/peerj.preprints.2137v1 | CC BY 4.0 Open Access | rec: 16 Jun 2016, publ: 16 Jun 2016

example, when vibrations occur near tanks or when sponges are moved. State 3 occurred more frequently at night, which was consistent with the depressed pumping rates at night (see below). State 3 also occurred several times per day following no direct stimulus. Adjacent oscula on the same individual were observed to open and close asynchronously, as shown for oscula 1 and 2 in Fig. 5.

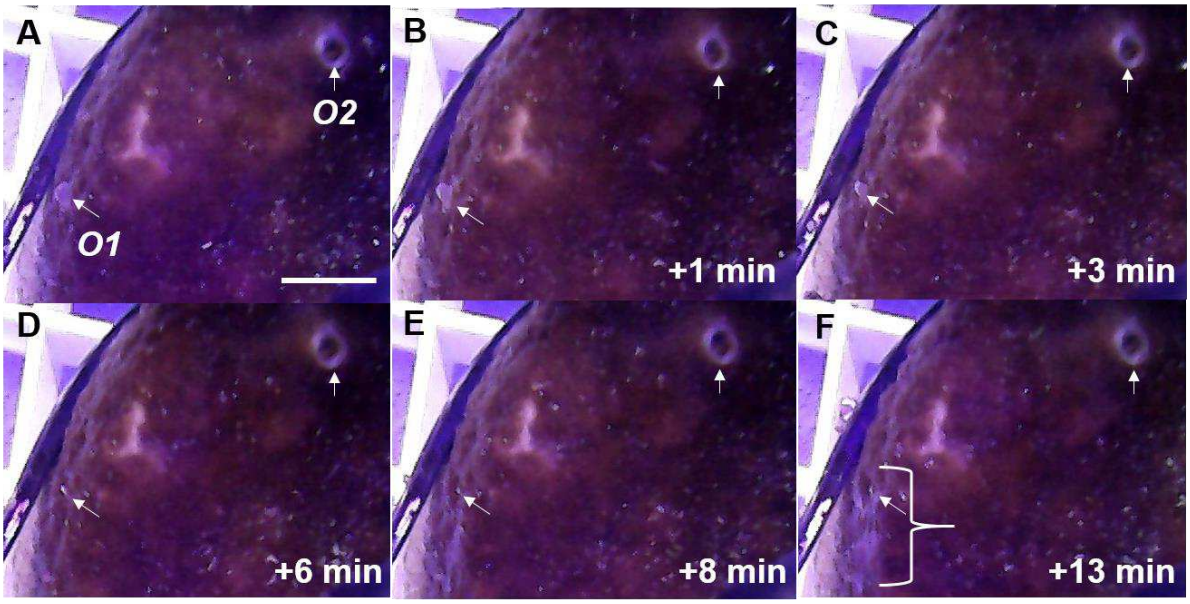

Figure 5. Time lapse images of *Cliona orientalis* oscular states. A. Both osculum one (O1) and osculum two (O2) were open with their papillae extended. B. O1 closed with papilla inflated. C. Contraction of the papilla of O1 (+ 3 min from B). D. Full retraction of the papilla of O1's papilla (+ 6 min). E. Area surrounding O1 starting to become concave (+11 min). F. Concave area at its most pronounced (bracketed region, + 16 min). No change was observed in O2 in this time series, demonstrating asynchrony among oscula states on an individual sponge.

Excurrent velocity was positively related to osculum area ($F_{1,123} = 120$, $R^2 = 0.495$, $P<0.01$). Excurrent velocities of an osculum measured for 10 mins in state 1 are shown in Fig. 1. The osculum contracted slightly during this time, but did not fully enter states 2 or 3. Osculum diameter was also tracked with excurrent velocity of a separate osculum on the same sponge as it entered state 3 (Fig. 6B), contracting the osculum and papilla. Excurrent

PeerJ Preprints | https://doi.org/10.7287/peerj.preprints.2137v1 | CC BY 4.0 Open Access | rec: 16 Jun 2016, publ: 16 Jun 2016

289 diameter correlated with osculum area ($F_{1,22}$ = 101, R^2 = 0.821, P < 0.01) with a higher R^2

290 value due to the active change in states observed.

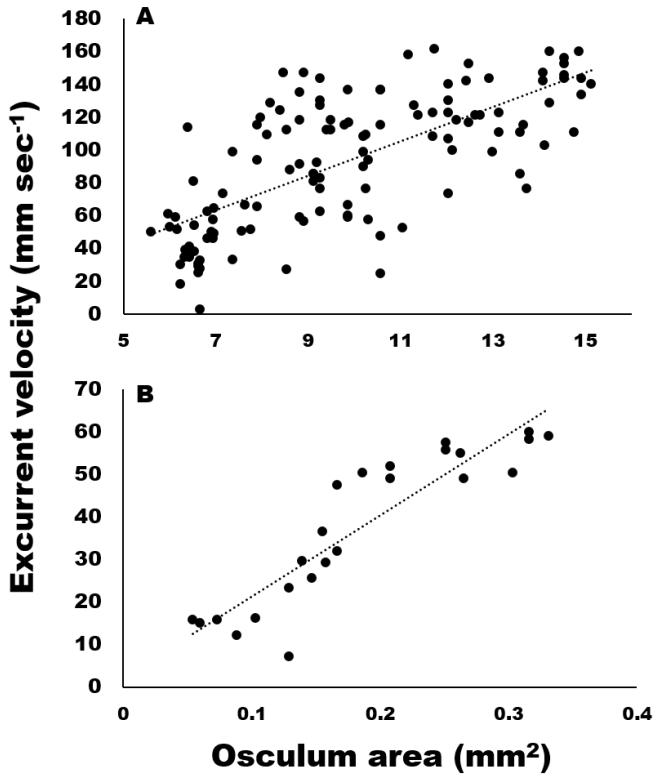

Figure 6. Excurrent velocity (mm s^{-1}) versus osculum area (mm^2). Osculum area was calculated from measured diameter, assuming a circular shape of the osculum. A. Osculum open to near capacity with small fluctuations in osculum area and pumping rate, i.e. oscular state 1. Excurrent velocity was directly correlated to osculum diameter ($F_{1,123}$ = 121, R^2 = 0.495, P < 0.01). B. A separate osculum on the same sponge was measured as it was closing, i.e. entering state 3. The two values were directly correlated ($F_{1,22}$ = 101, R^2 = 0.821, P < 0.01).

291 1.5 The effects of sediments on excurrent velocities

292 The single pulse of 100 mg L^{-1} sediment settled quickly, with SSC decreasing to ~50 mg L^{-1}

293 in the tanks after 1.5 h and ~40 mg L^{-1} after 3 h. Sedimentation rates during this time were 6

294 mg cm^{-2} day^{-1} (if normalised to a 24 h period). Immediately after exposure to the high SSC, 3

295 of the 4 sponges decreased excurrent velocities by 42–90%, and minimum velocities were

PeerJ Preprints | https://doi.org/10.7287/peerj.preprints.2137v1 | CC BY 4.0 Open Access | rec: 16 Jun 2016, publ: 16 Jun 2016

296 reached after 15 min (Fig. 7A). Following ~25 mins of reduced pumping rates, explant 1 and
297 2 increased their excurrent velocities. Explant 1 recovered velocities up to ~50% of pre-
298 treatment levels whereas explant 2 exhibited a short burst of high velocity post-treatment,
299 before reducing velocities to –50% of the pre-treatment level for ~80 mins, at which point
300 their oscula closed and pumping ceased. Explant 3 decreased pumping and then exhibited a
301 spike in excurrent velocity, however, it closed its osculum and pumping ceased after 30 min.
302 Although explant 4 did not exhibit a sharp decrease in excurrent velocity following exposure
303 to the elevated SSC, average velocity decreased by approximately 50% and osculum closure
304 and pumping cessation occurred after 180 min. All explants exhibited osculum closure and
305 pumping cessation after treatment. On average, the explants kept the oscula open for 99 ± 4
306 min (mean ± SD) after introduction of the sediment.

307

PeerJ Preprints | https://doi.org/10.7287/peerj.preprints.2137v1 | CC BY 4.0 Open Access | rec: 16 Jun 2016, publ: 16 Jun 2016

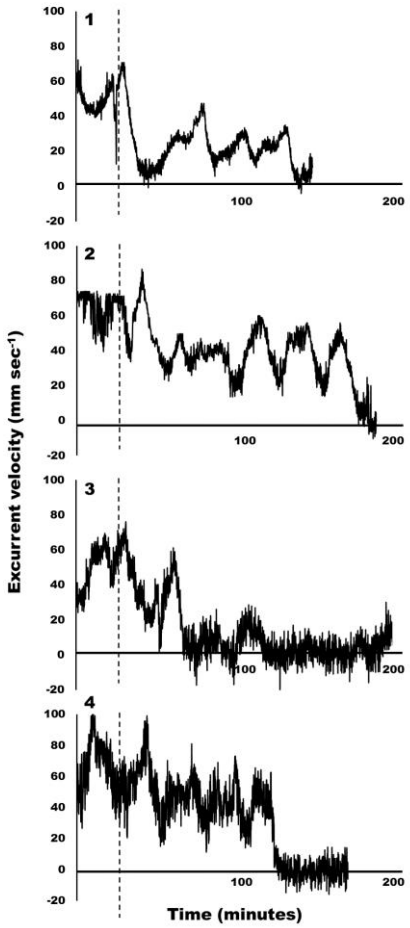

Figure 7. Excurrent velocities from four oscula of four separate explants exposed to a single dose of high SSC (100 mg L^{-1}), recorded using the thermistor flowmeter. The vertical, dashed line indicates when sediment was introduced. Measurements were ended when oscula contracted and excurrent velocities were zero. Small oscillations in ambient flow resulted in negative values when excurrent velocities were zero.

308

309 Excurrent velocities showed diel trends when monitored over several days. During the
310 first 24 h, and before suspended sediments were added, excurrent velocities oscillated in a
311 regular pattern for all four individuals. For explants 5 to 8 shown in Fig. 8A, excurrent
312 velocities increased towards midday, reaching a maximum around the time of highest light
313 intensity, and then decreased into the night. On the second day, excurrent velocities were

PeerJ Preprints | https://doi.org/10.7287/peerj.preprints.2137v1 | CC BY 4.0 Open Access | rec: 16 Jun 2016, publ: 16 Jun 2016

314 generally lower and the diel cycle was less obvious, although night-time velocities decreased

315 for all individuals.

316

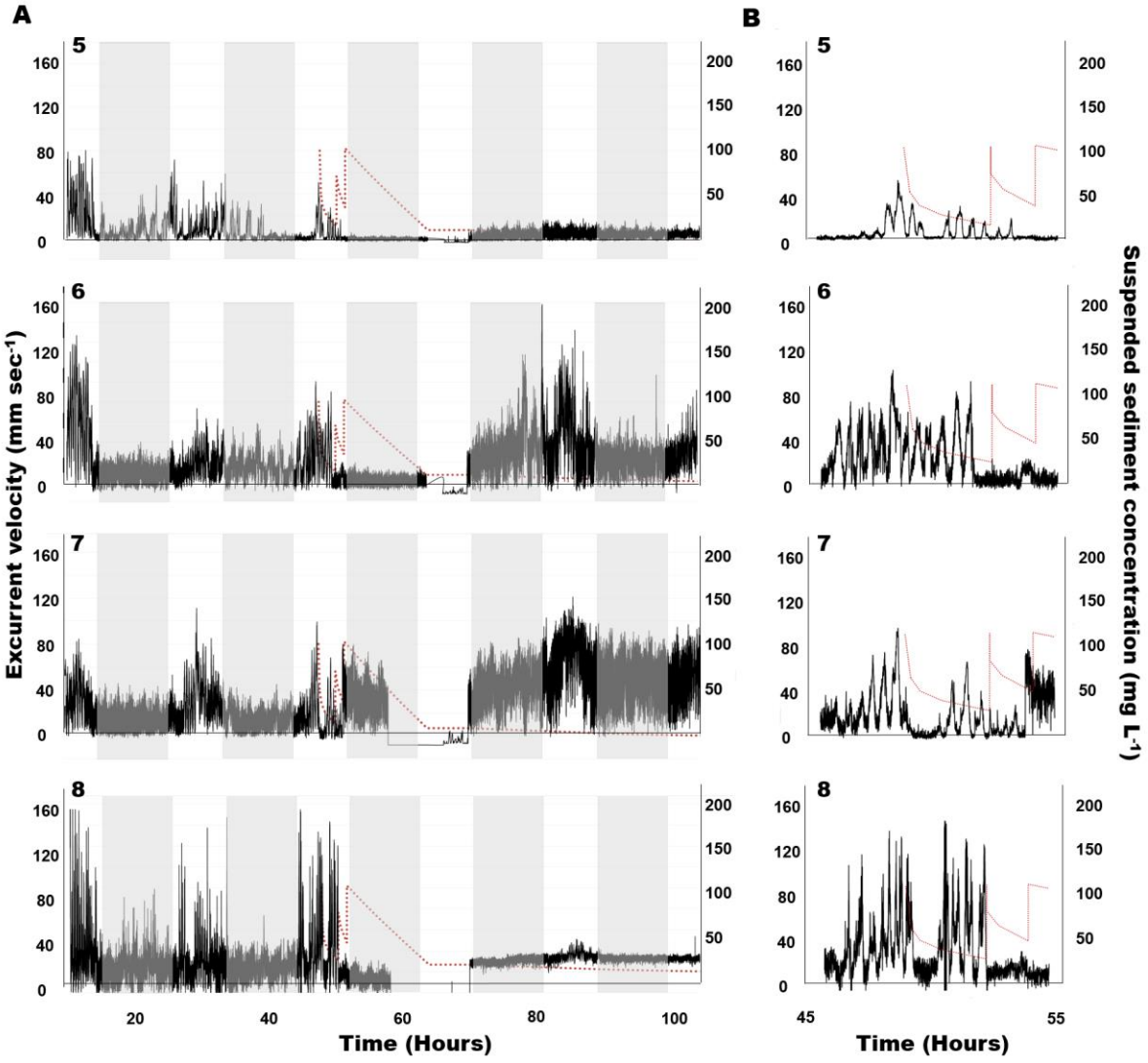

Figure 8. A. Pumping patterns in four *Cliona orientalis* over 5 d. The grey rectangles represent night. The red line on the third day represents suspended sediment concentrations (SSC) – see secondary y-axis. SSCs were not measured overnight and the line shown overnight was a linear estimate. Panels 5–8 represent a single osculum of different individual explants measured simultaneously. B. Close-up of the third day, when sediment was added. Excurrent velocities are shown in black and SSC are red.

317

PeerJ Preprints | https://doi.org/10.7287/peerj.preprints.2137v1 | CC BY 4.0 Open Access | rec: 16 Jun 2016, publ: 16 Jun 2016

Three pulses of sediment at 100 mg L^{-1} were added on the third day of recording with SSC shown in Fig. 8. The first sediment pulse reduced excurrent velocities for all measured oscula. Since pumping patterns oscillated regularly throughout the day, percentage change was recorded based on the maxima. Maximal excurrent velocity decreased by 41%, 11% and 36% for explants 4-7 respectively (mean: 29 ± 9%). In contrast, the maximal excurrent velocity of explant 8 increased by 7%. All four explants closed their oscula after the first sediment dose after an average of 56 ± 67 min. Explant 7 exhibited a very rapid closure, arresting pumping and closing after 6 min. All except explant 6 reopened their oscula and restarted pumping, albeit at lower excurrent velocities, before the second dose of sediment was added. For individuals 5, 7 and 8, oscula reopened and continued pumping 68 ± 26 mins after closure.

The second sediment dosing was administered after all oscula (except those of explant 6) had reopened and reinitiated pumping. Maximal excurrent velocities after the second dosing decreased by 59 ± 19% from pre-treatment maxima. However, variation was again detected between explants, with explant 5 ceasing pumping and closing its osculum after 70 mins, explant 6 keeping its osculum closed, explant 8 closing its osculum for <1 min, and explant 3 keeping its osculum open even after the second dose (although maximal excurrent velocity decreased by 39%).

After the third sediment dose, all individuals except explant 7 closed their oscula and ceased pumping until nightfall. Pumping ceased though the night, in concordance with the diel pumping pattern observed before treatment. Light attenuation caused by the sediment in the tanks was negligible (unpublished data), so the decreased pumping rates were not

PeerJ Preprints | https://doi.org/10.7287/peerj.preprints.2137v1 | CC BY 4.0 Open Access | rec: 16 Jun 2016, publ: 16 Jun 2016

attributed to a light cue. In contrast, explant 3 kept its oscula open although pumping velocity was reduced (Fig. 8). Approximately 48 h after the first sediment treatment, explants 6 and 7 had excurrent velocities similar to pre-treatment levels and the diel pattern was re-established with maximal excurrent velocities at peak light intensity. A similar pattern was observed in explant 8, although excurrent velocities did not return to pre-sediment levels. Explant 5 did not restart pumping or reopen its osculum for at least 72 h post-exposure to sediment.

Discussion

A four-channel, thermistor flowmeter with integrated video cameras was designed, constructed and validated in order to simultaneously measure sponge excurrent velocity and observe sponge behaviour. This instrument has an accuracy of ± 5 mm s^{-1} over the range of 5–200 mm s^{-1}, a spatial resolution of 1.4 mm, and a temporal resolution of 5 seconds. It is therefore suitable for many sponge species, particularly those with small oscula. Although the flowmeter is currently limited to experiments with constant water temperature, it has considerable utility for examining effects of environmental stress such as elevated SSCs and high sedimentation. Combining flowmeters with time lapse imagery yielded useful insights into sponge behaviour and facilitated a detailed assessment of the pumping rates of *Cliona orientalis* and the contractile states of its oscula. For *C. orientalis*, a positive correlation was established between osculum area and excurrent velocity. Diel fluctuations in pumping and oscula activity were observed, with increased pumping during the day and decreased pumping and oscula closure at night. Elevated SSCs decreased pumping rates and caused osculum contraction.

PeerJ Preprints | https://doi.org/10.7287/peerj.preprints.2137v1 | CC BY 4.0 Open Access | rec: 16 Jun 2016, publ: 16 Jun 2016

362 In order to describe the contractile behaviour, different osculum states were
363 examined. The area of the osculum when it was open with papilla extended, as well as the
364 transition from this state to a state of osculum closure with retracted papilla, correlated with
365 decreased excurrent velocity as measured by the thermistor flowmeter. Osculum area was
366 previously found to be directly correlated with excurrent velocity in *Tethya crypta* (de
367 Laubenfels, 1949; Reiswig, 1971). This correlation indicates that either the osculum acts as a
368 passive, elastic valve that closes when no pressure is applied by the pumping choanocytes or
369 that there is some communication between choanocytes and contractile pinacocytes in the
370 osculum. Observations of osculum state 2, wherein the osculum is closed but the papillae is
371 extended, demonstrated that the interaction between pumping and contraction was more
372 complex than a simple, passive valve. The osculum itself may now be considered a sensory
373 organ that coordinates behavioural responses, sensing and reacting to decreased pumping
374 by choanaocytes (Ludeman et al., 2014). Flow sensing ciliated pinacocytes have been
375 identified in oscula from numerous sponge species and classes (Hammel and Nickel, 2014;
376 Ludeman et al., 2014). Although flow sensing cilia structures have not yet been observed in
377 *C. orientalis*, it is likely that they are present given the results seen here. If so, then the
378 oscula of *C. orientalis* sense low flow from the choanocytes and then close in response. *C.*
379 *orientalis* has multiple oscula per individual that contract asynchronously under normal
380 conditions. Therefore, the level of connection and coordination among oscula on a single
381 sponge and, more importantly, the aquiferous system related to each osculum, remains to
382 be determined.

383 Maximal excurrent velocities increased during the day (peaking around noon) and
384 were minimal at night. This coincided with an observed decrease in osculum area at night.

PeerJ Preprints | https://doi.org/10.7287/peerj.preprints.2137v1 | CC BY 4.0 Open Access | rec: 16 Jun 2016, publ: 16 Jun 2016

385 The Caribbean sponge *Cliona varians* (Duchassaing & Michelotti 1864) also contracts its
386 oscula at night (Strehlow pers. obs.), as does *T. crypta*, which concurrently decreases its
387 excurrent velocity overnight (Reiswig, 1971). Fang et al. (2016) demonstrated that *C.*
388 *orientalis* increases its chemical bioerosion rate during the day as compared to the night.
389 Furthermore, the distribution of endosymbiotic *Symbiodinium* within *C. orientalis* changes
390 following a diel rhythm (Schönberg & Suwa, 2007; Fang et al., 2016). Changes in pumping
391 activity may be a central part of the diel rhythms of the *C. orientalis* holobiont, as pumping is
392 critical to feeding, gas exchange and waste elimination. However, a direct, causal link
393 between increased pumping rates, increased bioerosion and altered symbiont distribution
394 has yet to be established.

395 The contraction of the area surrounding the osculum (i.e. state 4) in *C. orientalis* is
396 analogous to the contractile 'epithelium' *sensu lato* noted in *Tethya wilhelma,* where the
397 entire pinacodermal surface exhibits regular contractile patterns during the day, with
398 contractile frequencies decreasing at night (Nickel et al., 2011). These contractions are
399 triggered locally and spread over the whole sponge surface, constricting the channels and
400 decreasing the sponge volume (Nickel et al., 2011). Fused individuals of *T. wilhelma* even
401 synchronise their contractions following grafting (Nickel, 2004; Nickel et al., 2011).

402 Elevated SSCs were found to decrease maximal excurrent velocities in *C. orientalis* by
403 30–90% after a single dose, ~67% after a second dose, and pumping was entirely arrested
404 following a second dose. All oscula on all sponges closed after the first dose of sediment,
405 while repeated doses caused longer closures. These reductions in pumping rates and
406 prolonged osculum closures are implicitly detrimental to sponges (see Bell et al., 2015).

PeerJ Preprints | https://doi.org/10.7287/peerj.preprints.2137v1 | CC BY 4.0 Open Access | rec: 16 Jun 2016, publ: 16 Jun 2016

Decreased pumping rates in response to elevated SSCs have been reported in numerous sponge species. In *Aplysina lacunosa* (Lamarck, 1814), pumping rates decrease by 41% after exposure to sediment concentrations of ~100 mg L^{-1} (Gerrodette & Flechsig, 1979) and oscula of *Tethya crypta* close rapidly in response to wave action and sand score, with storms causing pumping activity to drop by 27% (Reiswig, 1971). Similarly, *Rhabdocalyptus dawsoni* (Lambe, 1893) reduces pumping by 32% within five minutes after exposure to sediments and can also arrest pumping in response to mild tactile stimulation (Leys, Mackie & Meech, 1999; Tompkins-MacDonald & Leys, 2008). However, not all sponges are equally sensitive to tactile disturbance. The glass sponge *Aphrocallistes vastus* (Schulze, 1886) only arrested pumping when stabbed with a pipette (Tompkins-MacDonald & Leys, 2008). *A. vastus* does however react rapidly (within 2 seconds) to deposited sediment with cessation of pumping lasting for intervals of 30–40 seconds (Tompkins-MacDonald & Leys, 2008). These intervals are comparatively shorter than what was observed in *C. orientalis* and may be due to the ability of glass sponges to rapidly propagate action potentials across syncytial tissue (Leys, Mackie & Meech, 1999). *R. dawsoni* arrests pumping at lower sediment concentrations (~15 mg L^{-1}) than *A. vastus* (~36 mg L^{-1}) and when sediment levels are kept constant, pumping rates decreased by 50–80% and 5–70% in *A. vastus* and *R. dawsoni*, respectively. Pumping levels generally recovered after sediment addition stopped, but this process took 3–25 hours in *R. dawsoni* and approximately 6 hours in *A. vastus* (Tompkins-MacDonald & Leys, 2008). Differences in recovery times highlight the physiological variability of sponge species.

PeerJ Preprints | https://doi.org/10.7287/peerj.preprints.2137v1 | CC BY 4.0 Open Access | rec: 16 Jun 2016, publ: 16 Jun 2016

Conclusion

Acute exposures to elevated SSCs caused pumping rates to decrease by up to 90% in *C. orientalis*. This decrease was generally followed by a coordinated closure of the oscula and the cessation of pumping. The thermistor flowmeter apparatus developed here is a valuable tool for monitoring the behaviour and physiology of sponges exposed to environmental stressors.

Acknowledgments

We are thankful to SeaSim staff for their help during experiment set up. Many thanks to Dr. C.H.L. Schönberg for initial discussion and design input in the development of the thermistor flowmeter. Thanks also to Dr. M. Abdul Wahab for comments on a previous version of the manuscript. N.S.W was funded by an Australian Research Council Future Fellowship FT120100480.

Funding statement

This research was funded by the Western Australian Marine Science Institution (WAMSI) as part of the WAMSI Dredging Science Node, and made possible through investment from Chevron Australia, Woodside Energy Limited, BHP Billiton as environmental offsets and by co-investment from the WAMSI Joint Venture partners. The commercial entities had no role in data analysis, decision to publish, or preparation of the manuscript. The views expressed herein are those of the authors and not necessarily those of WAMSI.

PeerJ Preprints | https://doi.org/10.7287/peerj.preprints.2137v1 | CC BY 4.0 Open Access | rec: 16 Jun 2016, publ: 16 Jun 2016

References

Bell JJ., McGrath E., Biggerstaff A., Bates T., Bennett H., Marlow J., Shaffer M. 2015. Sediment impacts on marine sponges. *Marine Pollution Bulletin* 94:5–13. DOI: 10.1016/j.marpolbul.2015.03.030.

Elliott GRD., Leys SP. 2007. Coordinated contractions effectively expel water from the aquiferous system of a freshwater sponge. *The Journal of Experimental Biology* 210:3736–3748. DOI: 10.1242/jeb.003392.

Ellwanger K., Nickel M. 2006. Neuroactive substances specifically modulate rhythmic body contractions in the nerveless metazoon *Tethya wilhelma* (Demospongiae, Porifera). *Frontiers in zoology* 3:7. DOI: 10.1186/1742-9994-3-7.

Fang JKH., Schönberg CHL., Hoegh-Guldberg O., Dove S. 2016. Day–night ecophysiology of the photosymbiotic bioeroding sponge *Cliona orientalis* Thiele, 1900. *Marine Biology* 163:100. DOI: 10.1007/s00227-016-2848-4.

Field ME., Chezar H., Storlazzi CD. 2013. SedPods: A low-cost coral proxy for measuring net sedimentation. *Coral Reefs* 32:155–159. DOI: 10.1007/s00338-012-0953-5.

Gerrodette T., Flechsig AO. 1979. Sediment-induced reduction in the pumping rate of the tropical sponge *Verongia lacunosa*. *Marine Biology* 55:103–110. DOI: 10.1007/BF00397305.

Grant R. 1826. Notice of a New Zoophyte (*Cliona celata* Gr.) from the Firth of Forth. *Edinburgh New Philosophical Journal*:78–81.

Hammel JU., Nickel M. 2014. A new flow-regulating cell type in the Demosponge *Tethya wilhelma* - functional cellular anatomy of a leuconoid canal system. *PloS one* 9:e113153. DOI: 10.1371/journal.pone.0113153.

Harrison FW. 1972. Phase contrast photomicrography of cellular behaviour in spongillid porocytes (Porifera: Spongillidae). *Hydrobiologia* 40:513–517. DOI: 10.1007/BF00019986.

Ilan M., Abelson A. 1995. The life of a sponge in a sandy lagoon. *Biological Bulletin* 189:363–369. DOI: 10.2307/1542154.

Jones R., Fisher R., Stark C., Ridd P. 2015. Temporal patterns in seawater quality from dredging in tropical environments. *PLoS ONE* 10:e0137112. DOI: 10.1371/journal.pone.0137112.

Leys SP., Mackie GO., Meech RW. 1999. Impulse conduction in a sponge. *The Journal of experimental biology* 202:1139–1150.

Leys SP., Meech RW. 2006. Physiology of coordination in sponges. *Canadian Journal of Zoology* 84:288–306. DOI: 10.1139/z05-171.

Ludeman D a., Farrar N., Riesgo A., Paps J., Leys SP. 2014a. Evolutionary origins of sensation in metazoans : functional evidence for a new sensory organ in sponges.

Ludeman DA., Farrar N., Riesgo A., Paps J., Leys SP. 2014b. Evolutionary origins of sensation in metazoans: functional evidence for a new sensory organ in sponges. *BMC Evolutionary Biology* 14:1–11. DOI: 10.1186/1471-2148-14-3.

Mackie GO., Lawn ID., Pavans de Ceccatty M. 1983. Studies on hexactinellid sponges. II. Excitability, conduction and coordination of responses in *Rhabdocalyptus dawsoni* (Lambe, 1873*). Philos Trans R Soc Lond B Biol Sci* 301:401–418.

Massaro AJ., Weisz JB., Hill MS., Webster NS. 2012. Behavioral and morphological changes caused by thermal stress in the Great Barrier Reef sponge *Rhopaloeides odorabile*. *Journal of Experimental Marine Biology and Ecology* 416-417:55–60. DOI: 10.1016/j.jembe.2012.02.008.

McMurray SE., Pawlik JR., Finelli CM. 2014. Trait-mediated ecosystem impacts: how morphology and size affect pumping rates of the Caribbean giant barrel sponge. *Aquatic Biology* 23:1–13. DOI: 10.3354/ab00612.

Mendola D., van den Boogaart JGM., van Leeuwen JL., Wijffels RH. 2007. Re-plumbing in a Mediterranean sponge. *Biology letters* 3:595–598. DOI: 10.1098/rsbl.2007.0357.

Moore JP. 2003. A thermistor based sensor for flow measurement in water. *MSc Dissertation, School of Physical Sciences Dublin City University, Ireland.*

PeerJ Preprints | https://doi.org/10.7287/peerj.preprints.2137v1 | CC BY 4.0 Open Access | rec: 16 Jun 2016, publ: 16 Jun 2016

497 Nickel M. 2004. Kinetics and rhythm of body contractions in the sponge *Tethya wilhelma* (Porifera:
498 Demospongiae). *The Journal of experimental biology* 207:4515–4524. DOI: 10.1242/jeb.01289.

499 Nickel M., Scheer C., Hammel JU., Herzen J., Beckmann F. 2011. The contractile sponge epithelium sensu lato--
500 body contraction of the demosponge *Tethya wilhelma* is mediated by the pinacoderm. *The Journal of*
501 *experimental biology* 214:1692–1698. DOI: 10.1242/jeb.049148.

502 Reiswig HM. 1971. In situ pumping activities of tropical Demospongiae. *Marine Biology* 9:38–50. DOI:
503 10.1007/BF00348816.

504 Schläppy M-L., Weber M., Mendola D., Hoffmann F., de Beer D. 2010. Heterogeneous oxygenation resulting
505 from active and passive flow in two Mediterranean sponges, *Dysida avara* and *Chondrosia reniformis*.
506 *Limnology and Oceanography* 55:1289–1300. DOI: 10.4319/lo.2010.55.3.1289.

507 Schönberg CHL., Suwa R. 2007. Why bioeroding sponges may be better hosts for symbiotic dinoflagellates than
508 many corals. *Porifera research: biodiversity, innovation and sustainability* 28:569–580.

509 Schneider CA., Rasband WS., Eliceiri KW 2012. NIH Image to ImageJ: 25 years of image analysis. *Nature*
510 *methods* 9:671-675. PMID 22930834.

511 Tompkins-MacDonald GJ., Leys SP. 2008. Glass sponges arrest pumping in response to sediment: Implications
512 for the physiology of the hexactinellid conduction system. *Marine Biology* 154:973–984. DOI:
513 10.1007/s00227-008-0987-y.

514 Weissenfels N. 1976. Bau und Function des SuBwasserschwamms *Ephydatia fluviatilis* L. (Porifera),
515 Nahrungsaufnahme, I I I, Verdauung und Defaekation. *Zoomorphologie* 85:73–88.

516 Weisz JB., Lindquist N., Martens CS. 2008. Do associated microbial abundances impact marine demosponge
517 pumping rates and tissue densities? *Oecologia* 155:367–376. DOI: 10.1007/s00442-007-0910-0.

PeerJ Preprints | https://doi.org/10.7287/peerj.preprints.2137v1 | CC BY 4.0 Open Access | rec: 16 Jun 2016, publ: 16 Jun 2016